Peertechz

Open Journal of Chemistry

submitpaper@peertechz.com

CHEMISTRY GROUP

Open Journal of Chemistry

ISSN: 2641-3051 DOI: https://dx.doi.org/10.17352/ojc

Review Article

On population-space description of chemical reactivity

Roman F Nalewajski*

Department of Theoretical Chemistry, Jagiellonian University, Gronostajowa 2, 30-387 Cracow, Poland

Received: 20 May, 2024
Accepted: 30 May, 2024
Published: 31 May, 2024

***Corresponding author:** Roman F Nalewajski, Department of Theoretical Chemistry, Jagiellonian University, Gronostajowa 2, 30-387 Cracow, Poland,
E-mail: nalewajs@chemia.uj.edu.pl

ORCiD: https://orcid.org/0009-0009-9630-8045

Keywords: Acid-base complexes; Charge-transfer reactivity; Chemical hardness and softness; Intersecting-state model; *In situ* descriptors; Reaction-energy profiles

Copyright: © 2024 Nalewajski RF. This is an open-access article distributed under the terms of the Creative Commons Attribution License, which permits unrestricted use, distribution, and reproduction in any medium, provided the original author and source are credited.

https://www.chemisgroup.us

Check for updates

Abstract

The electron-population degrees-of-freedom of donor-acceptor systems are reexamined and alternative simple models of charge-transfer reactivity are discussed in the substrate and atomic resolutions. The *in situ* differential descriptors of the polarized subsystems are emphasized and alternative energy profiles in interactions between hard and soft acidic and basic reactants are used to investigate the process representative activation and reaction energies. The intersecting-state model of such acid-base (AB) systems is explored, its predictions of the reaction transition-state complex and its properties are summarized, and composite $(AB)_n$ systems are commented upon.

Introduction

The advent of Density Functional Theory (DFT) [1-6] has brought a renewed interest in molecular electron densities and the associated "population" degrees of freedom as primary descriptors of the mechanism and progress of elementary chemical reactions [7-16]. This also covers the probabilistic models of the chemical bond in Information Theory (IT) [16,17] in all resolution levels of electronic distributions, from the *local* description of densities themselves to *intermediate* descriptions of the overall electron numbers in molecular substrates, their active sites or constituent atoms. For example, such "condensed" descriptions may involve occupation numbers of the configuration Molecular Orbitals (MO) or probability data regarding the adopted definition of bonded Atoms-in-Molecules (AIM) or specific basis set of Atomic Orbitals (AO) used in molecular calculations.

The most condensed level, of a *global* description in terms of the average electron numbers on reactants, requires an identification of the *in situ* reactivity criteria for an (isoelectronic) charge-transfer (CT) phenomena in the *externally*-closed reactive system as a whole [9,11,12,16-18], e.g., in the *acid* (A, acceptor) — *base* (B, donor) (AB) complexes. A determination of the optimum amount of such "concerted" displacements in overall electron populations and the subsequent equilibrium responses of reactants, involves the reaction *chemical potential* (gradient) and *hardness* (Hessian) descriptors. Their known *finite*-difference estimates, used in qualitative considerations, e.g., [4,9-13,19], ultimately refer to the substrate ionization-potential (I_α) and electron-affinity (A_α) properties. In this work, we reexamine definitions of the proper CT descriptors of the closed and open reactants, all of which can be determined from the canonical data on the system constituent AIM [9,10].

The population reference systems of the substrates have to be mutually oriented in an AIM-resolved reaction mechanism. In the *Intersecting-State Model* (ISM) [10-12] this has been accomplished by requiring *collinearity* of the reactant internal Fukui Functions (FF), each reflecting the populational "trajectory" of the most efficient mode of an electron "inflow" or "outflow" to/from the molecular fragment in question. The ISM perspective has also anticipated a lowering of the process activation energy upon an external "opening" of the reactive system in contact with an electron reservoir, e.g., the (macroscopic) catalytic surface. In the present analysis, we shall summarize these conjectures and briefly explore the possibility of supramolecular assemblies of the bonded AB monomers.

Charge-transfer in reactant resolution

Let us briefly reexamine the populational derivatives characterizing a general CT reactive system R ≡ A—B. We aim to describe the *internal* (isoelectronic) transfer of the equilibrium amount of N_{CT} electrons between the initially *closed* reactants in the nonequilibrium (nonbonded) complex $R^+ = (A^+|B^+)$, from the polarized "donor" reactant B^+ to its "acceptor" partner A^+,

$$dN_A = -dN_B = N_{CT} > 0 \text{ or } dN_R \equiv dN_A + dN_B = 0, \qquad (1)$$

for the fixed *molecular* external potential $v(\boldsymbol{r}) = v_A(\boldsymbol{r}) + v_B(\boldsymbol{r})$, corresponding to the "frozen" geometry of R as a whole. The optimum CT flow ultimately produces the equilibrium (bonded) complex $R^* = (A^*¦B^*)$ (Figure 1). The vertical *solid* and *broken* lines in R^+ and R^*, respectively, symbolize the "barrier" and "freedom" to exchange electrons between the externally-closed reactants [9-12]. For simplicity, we further assume that internal geometries of the isolated reactants A^0 and B^0 are held frozen in the reaction complex, so that there exists a unique "molecular" reference $R^0 \equiv (A^0|B^0)$, consisting of the free reactants shifted to their current mutual orientation and separation in R. Again, the vertical solid line separating the nonbonded fragments of R^0 implies that they both conserve their initial electron numbers, when polarized by a presence of the other subsystem: $N_\alpha^{\,0} = N_\alpha^{\,+}$, α = A, B.

Such an internal transfer of N_{CT} electrons in R^*, between the already polarized reactants of $R^+ \equiv (A^+|B^+)$, thus conserves the complex overall number of electrons: $N_A + N_B \equiv N_R$. The equilibrium electron populations on subsystems, $\boldsymbol{N}^* = (N_A^{\,*}, N_B^{\,*})$, which directly result from integrations of the associated fragment densities $\boldsymbol{\rho}^* = (\rho_A^{\,*}, \rho_B^{\,*})$,

$$N_\alpha^{\,*} = \int \rho_\alpha^{\,*}(\boldsymbol{r})\, d\boldsymbol{r},\ \alpha = A, B;$$

$$\boldsymbol{N}^* \equiv \boldsymbol{N}^0 + \Delta\boldsymbol{N}^*(N_{CT}) = (N_A^{\,*} = N_A^{\,0} + N_{CT},\ N_B^{\,*} = N_B^{\,0} - N_{CT}), \qquad (2)$$

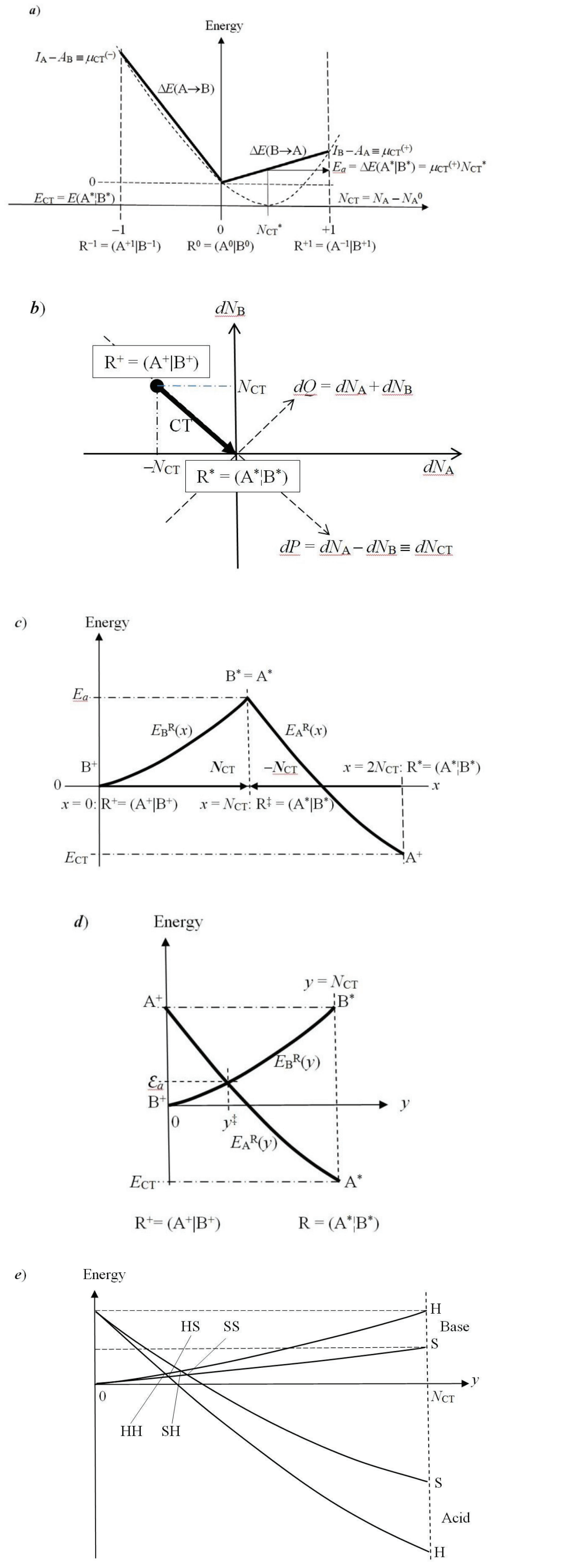

Figure 1: The *internal* CT process in a reactive system R = A—B combines the acceptor (acid, A) and donor (base, B) substrates. *Panel a*: chemical potential discontinuity and the system CT activation; *Panel b*: displacements in subsystem populations and normal modes for charge reorganizations in the open system; *Panel c*: energy profile for the bond-formation reaction along the isoelectronic (*N*-restricted) CT process $(A^+|B^+) \to (A^*|B^*) \to (A^*¦B^*)$; *Panel d*: juxtaposed energy plots for the "basis-activation" and "acid-stabilization" along the progress variable *y* measuring the current amount of B→A CT; *Panel e*: transition-state analysis of the Hard (H) and Soft (S) acids and bases.

Citation: Nalewajski RF (2024) On population-space description of chemical reactivity. Open Journal of Chemistry 10(1): 047-057.
DOI: https://dx.doi.org/10.17352/ojc.000039

Ultimately determine the optimum amount of the B→A CT:

$$N_{CT} = N_A^{\ *} - N_A^{\ 0} = N_B^{\ 0} - N_B^{\ *} > 0 \text{ or } \Delta\mathbf{N}^*(N_{CT}) = N_{CT}(1, -1). \qquad (3)$$

Here, the row vector $\mathbf{N}^0 = (N_A^{\ 0}, N_B^{\ 0})$ groups the electron populations of the reference (free or polarized) reactants in *non*-bonded complexes R^0 or R^+.

The equilibrium densities $\boldsymbol{\rho}^+(\mathbf{N}_R^{\ +})$ and energies $E^+(\mathbf{N}_R^{\ +})$ of the *externally* open but *mutually* closed reactants in the composite macroscopic system involving *separate* electron reservoirs for each substrate, $\mathbf{M}^+ \equiv (\mathbf{R}_A ¦ A^+|B^+ ¦ \mathbf{R}_B)$, thus depend on their current (average) electron populations $\mathbf{N}_R^{\ +} = \{N_\alpha^{\ +}\}$ ("row" vector), giving rise to overall (average) electron number in R^+ as a whole: $N_R^{\ +} = \sum_\alpha N_\alpha^{\ +}$. These functions ultimately determine charge sensitivities of the "embedded", polarized reactants $\{\alpha^+\}$, including the (row vector) of the *chemical potentials* in polarized subsystems,

$$\boldsymbol{\mu}_R^{\ +} = \partial E^+(\mathbf{N}_R^{\ +})/\partial \mathbf{N}_R^{\ +} = \{\mu_\alpha = \partial E^+(\mathbf{N}_R^{\ +})/\partial N_\alpha^{\ +}\}, \qquad (4)$$

and the *hardness matrix* in this reactant resolution:

$$\boldsymbol{\eta}_R^{\ +} = \partial^2 E^+(\mathbf{N}_R^{\ +})/\partial \mathbf{N}_R^{\ +}\partial \mathbf{N}_R^{\ +} = \{\eta_{\alpha,\beta} = \partial^2 E^+(\mathbf{N}_R^{\ +})/\partial N_\alpha^{\ +}\partial N_\beta^{\ +} = \partial\mu_\beta^{\ +}/\partial N_\alpha^{\ +}\}. \qquad (5)$$

In this "condensed" resolution the overall fragment populations $\mathbf{N}_R = (N_A, N_B) = \{N_\alpha\}$ represent the system independent electronic-structure variables, which determine the populational derivatives of reactants: their chemical potentials $\boldsymbol{\mu}_R = \partial E_R(\mathbf{N}_R)/\partial \mathbf{N}_R = \{\mu_\alpha\}$ and hardness matrix $\boldsymbol{\eta}_R = \partial^2 E_R(\mathbf{N}_R)/\partial \mathbf{N}_R\,\partial \mathbf{N}_R = \partial\boldsymbol{\mu}_R/\partial \mathbf{N}_R = \{\eta_{\alpha,\beta}\}$. The fragment populations combine into the *normal* coordinates describing R as a whole: polarization, $P = N_A - N_B$, and CT, $Q = N_A + N_B \equiv N_R$. In such a *collective* representation the system *internal* (isoelectronic) CT is thus directed along the polarization coordinate P, by the population shift $N_{CT} = (N_{CT}, -N_{CT})$ of the "*closed-to-open*" transition $R^+ \equiv (A^+|B^+) \longrightarrow R^* \equiv (A^* ¦ B^*)$, which corresponds to the vanishing *external*-CT displacement: $dQ = 0$. This CT process results in stabilization energy $\Delta E(N_{CT}) \equiv E_{CT} < 0$ and requires the population-activation of the *mutually*-closed (equilibrium) subsystems: $\Delta E(A^a|B^a) \equiv E_a = E(A^*|B^*) - E(A^+|B^+) = \mu_{CT}^{\ (+)} N_{CT}^{\ *} > 0$. In Panel *C* the reaction energy profile along the CT coordinate x consists of the "basis-activation" curve, $E_B^{\ R}(x) = -\mu_B x + \frac{1}{2}\eta_B^{\ R} x^2$, for $0 \le x \le N_{CT}$, followed by the "acid-stabilization" function, $E_A^{\ R}(x) = \mu_A x + \frac{1}{2}\eta_A^{\ R} x^2$, for $N_{CT} \le x \le 2N_{CT}$, with a common value $E_A^{\ R}(x^\ddagger)$ $E_B^{\ R}(x^\ddagger) \equiv E_a = E(A^*|B^*)$ in the *transition-state* (TS) at $x^\ddagger = N_{CT}$. These two energy segments are juxtaposed in Panel *d* as functions of the CT-progress variable $y \in [0, N_{CT}]$. Their intersection determines the representative amount of CT "activation", $0 \le y^\ddagger \equiv \mathbf{N}_{CT} \le N_{CT}$, and the associated energy: $E_a = E_A^{\ R}(y^\ddagger) = E_B^{\ R}(y^\ddagger)$.

These condensed descriptors define the associated *second*-order expansion of electronic energy in terms of powers of displacements in overall populations on subsystems,

$$\Delta E^+(\Delta\mathbf{N}_R^{\ +}) = \Delta\mathbf{N}_R^{\ +}\,(\partial E^+/\partial\mathbf{N}_R^{\ +}) + \tfrac{1}{2}\,\Delta\mathbf{N}_R^{\ +}\,[\partial^2 E^+/\partial\mathbf{N}_R^{\ +}\,\partial\mathbf{N}_R^{\ +}]\,\Delta\mathbf{N}_R^{\ +,T}$$

$$= \Delta\mathbf{N}_R^{\ +}\boldsymbol{\mu}_R^{\ +,T} + \tfrac{1}{2}\,\Delta\mathbf{N}_R^{\ +}\boldsymbol{\eta}_R^{\ +}\Delta\mathbf{N}_R^{\ +,T}. \qquad (6)$$

In the fixed (molecular) external potential $v(\mathbf{r})$ of the Born-Oppenheimer (BO) approximation, for the equilibrium amount N_{CT} of CT in $R^*(N_{CT})$, $\mathbf{N}_R(N_{CT}) = \{N_\alpha^{\ *}(N_{CT})\}$, a similar population-dependence characterizes the electron densities and energy of the mutually-open (bonded) reactants, in the composite macroscopic system involving a *common* electron reservoir for both substrates, $M^* \equiv (R ¦ A^* ¦ B^*) = (R ¦ R^*)$,

$$\boldsymbol{\rho}^*[\mathbf{N}_R(N_{CT});\, v] = \boldsymbol{\rho}_R(N_{CT}),\ E^*[\mathbf{N}_R(N_{CT});\, v] = E_R[\mathbf{N}_R(N_{CT})] \equiv E(N_{CT}). \qquad (7)$$

The equilibrium amount of CT thus represents the reaction coordinate, a progress variable in such *internal* displacements of the system's electronic structure. The associated *in situ* descriptors then involve differentiations concerning this amount of B→A CT [9-12,16-18]. The closure relation of Eq. (1) implies the following populational derivatives of reactants along this internal CT coordinate, generating the *row*-vector of their FF indices

$$\mathbf{F}_R^{\ CT} = \partial\mathbf{N}_R/\partial N_{CT} = (F_A^{\ CT}, F_B^{\ CT}),\ \textstyle\sum_\alpha F_\alpha^{\ CT} = 0;$$

$$F_A^{\ CT} = \partial N_A^{\ +}(N_{CT})/\partial N_{CT} = 1 \text{ and } F_B^{\ CT} = \partial N_B^{\ +}(N_{CT})/\partial N_{CT} = -1. \qquad (8)$$

These "condensed" subsystem indices enter as "weighting" factors into the *chain*-rule expressions for the relevant *in situ* CT descriptors. For example, the CT chemical-potential displacement, the energy-conjugate of N_{CT},

$$\mu_R^{\ CT} = \partial E(N_{CT})/\partial N_{CT} = \textstyle\sum_\alpha (\partial N_\alpha^{\ +}/\partial N_{CT})\,(\partial E^+/\partial N_\alpha^{\ +})$$

$$= \textstyle\sum_\alpha F_\alpha^{\ CT}\mu_\alpha = \mathbf{F}_R^{\ CT}\boldsymbol{\mu}_R^{\ +,T}$$

$$= F_A^{\ CT}[\partial E^+(\mathbf{N}_R)/\partial N_A] + F_B^{\ CT}[\partial E^+(\mathbf{N}_R)/\partial N_B] = \mu_A - \mu_B, \qquad (9)$$

measures the initial difference of chemical potentials in the "embedded" (polarized) subsystems of R^+ and represents the driving force for the subsequent bond-formation process. The associated CT-hardness measure similarly reads:

$$\eta_R^{\ CT} = \partial^2 E(N_{CT})/(N_{CT})^2 = \textstyle\sum_\alpha\sum_\beta (\partial N_\alpha^{\ +}/N_{CT})\,(\partial^2 E^+/\partial N_\alpha^{\ +}\partial N_\beta^{\ +})\,(\partial N_\beta^{\ +}/N_{CT})$$

Citation: Nalewajski RF (2024) On population-space description of chemical reactivity. Open Journal of Chemistry 10(1): 047-057.
DOI: https://dx.doi.org/10.17352/ojc.000039

$= \sum_\alpha \sum_\beta F_\alpha^{\ CT} \eta_{\alpha,\beta} F^{CT} = \boldsymbol{F}_R^{\ CT} \boldsymbol{\eta}_R^{\ +} \boldsymbol{F}_R^{\ CT,T}$

$$= (\eta_{A,A} - \eta_{A,B}) + (\eta_{B,B} - \eta_{B,A}) \equiv \eta_A^{\ R} + \eta_B^{\ R}. \qquad (10)$$

Here, $\eta_\alpha^{\ R}$ denotes the effective hardness of the "embedded" fragment α^+ in R^+. Thus, at finite separations, the hardness descriptors of chemically interacting reactants, reflecting the presence of complementary subsystem $\beta \neq \alpha$ (a finite electron "reservoir"), which effectively softens the fragment α, are modified by a finite *off*-diagonal hardness

$$\eta_{\beta,\alpha} = \partial^2 E^+(\boldsymbol{N}_R^{\ +})/\partial N_\beta^{\ +} \partial N_\alpha^{\ +} = \partial \mu_\alpha^{\ +}(\boldsymbol{N}_R^{\ +})/\partial N_\beta^{\ +}.$$

The *in situ* CT-softness descriptor is then accordingly defined as the inverse of the above global CT-hardness index:

$$S_R^{\ CT} = \partial N_{CT}/\partial \mu_{CT} = \partial N_A^{\ CT}/\partial \mu_{CT} = -N_B^{\ CT}/\partial \mu_R^{\ CT} = 1/\eta_R^{\ CT}. \qquad (11)$$

These combined descriptors ultimately determine the associated 2nd-order change in electronic energy, $\Delta E(N_{CT})$, due to the internal displacement in the Donor-Acceptor (DA) reactive system R = AB,

$\Delta E(N_{CT}) = \mu_R^{\ CT} N_{CT} + ½\, \eta_R^{\ CT} (N_{CT})^2$

$$= [\mu_A N_{CT} + ½ \eta_A^{\ R} (N_{CT})^2] + [-\mu_B N_{CT} + ½ \eta_B^{\ R} (N_{CT})^2] \equiv \sum_\alpha \Delta E_\alpha(N_{CT}), \qquad (12)$$

the sum of reactant contributions $\{\Delta E_\alpha(N_{CT})\}$.

The equilibrium condition, of the vanishing CT gradient of electronic energy at R^*,

$$\partial E(N_{CT})/\partial N_{CT}|^* = \mu_R^{\ CT}(N_{CT}^{\ *}) \equiv \mu_A(N_{CT}^{\ *}) - \mu_B(N_{CT}^{\ *}) = {}_R^{\ CT} + \eta_R^{\ CT} N_{CT}^{\ *} = 0, \qquad (13)$$

then yields the optimum amount $N_{CT}^{\ *}$ of CT (Figure 1*a*),

$$N_{CT}^{\ *} = -\mu_R^{\ CT}/\eta_R^{\ CT} > 0, \qquad (14a)$$

$$\Delta E(N_{CT}^{\ *}) \equiv E_{CT}(N_{CT}^{\ *}) - E_{CT}(N_{CT} = 0) = -½ (\mu_R^{\ CT})^2/\eta_R^{\ CT} \equiv E_{CT}, \qquad (14b)$$

for which the chemical potentials of both reactants equalize at the molecular level

$\mu_R = \sum_\alpha (\partial E_R/\partial N_\alpha)(\partial N_\alpha/\partial N_R) \equiv \sum_\alpha \mu_\alpha f = \mu_A (\eta_B^{\ R}/\eta_{CT}) + \mu_B (\eta_A^{\ R}/\eta_{CT})$

$= \mu_A^{\ *} = \mu_A + \eta_A^{\ R} N_{CT}^{\ *} \equiv \mu_A(N_{CT}^{\ *})$

$$= \mu_B^{\ *} = \mu_B - \eta_B^{\ R} N_{CT}^{\ *} \equiv \mu_B(N_{CT}^{\ *}). \qquad (15)$$

The CT activation energy E_a of Figure 1*a* is determined by the equilibrium population shifts in the mutually closed, population-activated reactants $\{\alpha^a\}$ in contact with their respective reservoirs: $N_A^{\ *} = N_A^{\ 0} + N_{CT}^{\ *}$ and $N_B^{\ *} = N_B^{\ 0} - N_{CT}^{\ *}$. These displacements are effected by appropriate exchanges with the separate (macroscopic) reservoirs of subsystems in the composite polarized system $M^+ \equiv (R_A \vert A^+ | B^+ \vert R_B)$:

$$E_a = E(A^* | B^*) - E(A^+ | B^+) \equiv \Delta E(A^a | B^a). \qquad (16)$$

Summing the energy changes of such populationally-activated subsystems in the B→A CT then gives:

$E_a = \Delta E(A^a) + \Delta E(B^a) = [\mu_A^{\ +} N_{CT}^{\ *} + \mu_B^{\ +} (N_{CT}^{\ *})]$

$$= (I_B - A_A) N_{CT}^{\ *} \equiv \mu_{CT}^{\ (+)} N_{CT}^{\ *} > 0, \qquad (17)$$

where A_α and I_α stand for the electron affinity and ionization potential of reactant α, respectively, while

$$\mu_{CT}^{\ (+)} = I_B - A_A = \mu_{CT}(B \rightarrow A) > 0 \qquad (18)$$

denotes the *biased* chemical-potential difference [16] for the "positive" B→A CT in Figure 1*a*. It should be recalled, that the chemical potential μ in Eq. (9) represents the *unbiased* descriptor of chemical species, when we have no information about its action in the reactive complex.

In Mulliken's (M) interpolation [19] it is expressed by the arithmetic average of the system *acidic* (anionic, acceptor), ${}_\alpha^{\ (-)} = -I_\alpha$, and *basic* (cationic, donor), $\mu_\alpha^{\ (+)} = -A_\alpha$, measures,

$$\mu^{(M)} = ½\, [\mu_\alpha^{\ (-)} + \mu_\alpha^{\ (+)}] = -½\, (I_\alpha + A). \qquad (19)$$

Therefore, in this finite-difference estimate (Figure 1*a*)

$$\mu_{CT}^{\ (M)} = \mu_A^{\ (M)} - \mu_B^{\ (M)} = ½\, [\mu_{CT}^{\ (+)} - \mu_{CT}^{\ (-)}], \qquad (20)$$

where the *biased* chemical-potential difference for the ("negative") A→B CT in Figure 1*a*

$$\mu_{CT}^{\ (-)} = I_A - A_B \equiv \mu_{CT}(A \rightarrow B) > 0. \qquad (21)$$

The *biased* measures reflect the (macroscopic) chemical-potential discontinuity [20].

The "weighting" factors of the substrate chemical potentials $\boldsymbol{\mu}_R^{\ +} = \{\mu_\alpha\}$ in the *combination*-rule of Eq. (15) represent the *external* FF indices in R,

$$\boldsymbol{f}_R = \{f_A = \partial N_A/\partial N_R = \eta_B^{\ R}/\eta_{CT}, f_B = N_B/\partial N_R = \eta_A^{\ R}/\eta_{CT}\}, \qquad (22)$$

measuring responses in populations of complementary subsystems to an inflow ($dN = dN_R > 0$) or outflow ($dN = -dN_R < 0$) of electrons to/from the equilibrium complex $R^* = (A^* \vert B^*)$. The global hardness of R^* as a whole, $\eta_R = \partial^2 E_R(N_R)/\partial N_R^{\ 2}$, similarly reflects the external N_R-derivative of the system resultant chemical potential,

$\eta_R = \partial \mu_R/\partial N_R = \sum_\beta \sum_\alpha (\partial N_\beta/\partial N_R)(\partial \mu_\alpha/\partial N_\beta) f_\alpha = \sum_\beta \sum_\alpha f_\beta\, \eta_{\beta,\alpha} f_\alpha$

Citation: Nalewajski RF (2024) On population-space description of chemical reactivity. Open Journal of Chemistry 10(1): 047-057.
DOI: https://dx.doi.org/10.17352/ojc.000039

$$= (\eta_{A,A}\eta_{B,B} - \eta_{A,B}\eta_{B,A})/\eta_R^{CT} \equiv D(\boldsymbol{\eta}_R^{+})/\eta_R^{CT}, \quad (23)$$

where $D(\boldsymbol{\eta}_R^{+})$ stands for the determinant of the hardness matrix $\boldsymbol{\eta}_R^{+}$. The inverse of this *population*-Hessian measures the global softness of R*:

$$S_R = \partial N_R/\partial\mu_R = \eta_R^{CT}/D(\boldsymbol{\eta}_R^{+}). \quad (24)$$

Let us now examine in more detail the alternative indices of the relative-softness (FF) quantities in the DA reactive complex R = A—B. One observes that derivatives of Eq. (8) represent the overall FF indices of reactants for an isoelectronic (*internal*) CT, in an *externally*-closed R. This conservation of the overall number of electrons is indeed reflected by their vanishing sum:

$$F_A^{CT} + F_B^{CT} = (\partial N_R/\partial N_{CT})_N = 0. \quad (25)$$

The "condensed" descriptors of reactants result from an integration of the associated "local" FF in substrate resolution, $\boldsymbol{f}^{CT}(\boldsymbol{r}) = \{f_\alpha^{CT}(\boldsymbol{r}) = \partial N_\alpha/\partial N_{CT}\}$,

$$\int f_A^{CT}(\boldsymbol{r})\, d\boldsymbol{r} = \partial N_A/\partial N_{CT} = F_A^{CT}, \int f_B^{CT}(\boldsymbol{r})\, d\boldsymbol{r} = \partial N_B/\partial N_{CT} = F_B^{CT}.$$

The latter also follow the appropriate *chain* rules:

$$f_A^{CT}(\boldsymbol{r}) = \partial\rho_A(\boldsymbol{r})/\partial N_{CT} = \textstyle\sum_\alpha [\partial\rho_A(\boldsymbol{r})/\partial N_\alpha]\, F_\alpha^{CT}$$

$$= \partial\rho_A(\boldsymbol{r})/\partial N_A - \partial\rho_A(\boldsymbol{r})/\partial N_B \equiv f_{A,A}(\boldsymbol{r}) - f_{B,A}(\boldsymbol{r}), \quad (26)$$

$$f_B^{CT}(\boldsymbol{r}) = \partial\rho_B(\boldsymbol{r})/\partial N_{CT} = \textstyle\sum_\alpha [\partial\rho_B(\boldsymbol{r})/\partial N_\alpha]\, F_\alpha^{CT}$$

$$= \partial\rho_B(\boldsymbol{r})/\partial N_A - \partial\rho_B(\boldsymbol{r})/\partial N_B \equiv f_{A,B}(\boldsymbol{r}) - f_{B,B}(\boldsymbol{r}). \quad (27)$$

These local responses on reactants give rise to the overall *in situ* FF of R as a whole:

$$f_R^{CT}(\boldsymbol{r}) = \partial\rho_R(\boldsymbol{r})/\partial N_{CT} = \partial\rho_A(\boldsymbol{r})/\partial N_{CT} + \partial\rho_B(\boldsymbol{r})/\partial N_{CT} = f_A^{CT}(\boldsymbol{r}) + f_B^{CT}(\boldsymbol{r}),$$

$$\int f_R^{CT}(\boldsymbol{r})\, dr = F_A^{CT} + F_B^{CT} = 0. \quad (28)$$

To conclude this section, let us briefly summarize the softness and FF indices of the (nonbonded) composite reactive system $R^+ = (A^+|B^+)$, expressed in terms of elements in $\boldsymbol{\eta}_R^{+}$. The inverse of the "condensed" hardness matrix, $\boldsymbol{\eta}_R^{+} = \{\eta_{\alpha,\beta}\}$, $\alpha, \beta \in$ (A, B), which determines the determinant $D(\boldsymbol{\eta}_R^{+}) = \eta_{A,A}\eta_{B,B} - \eta_{A,B}\eta_{B,A} \equiv D$, ultimately defines the softness matrix

$$\boldsymbol{\sigma}_R^{+} = \partial\boldsymbol{N}_R^{+}/\partial\boldsymbol{\mu}_R^{+} = (\boldsymbol{\eta}_R^{+})^{-1} = \{S_{\alpha,\beta}\},$$

$$\begin{bmatrix} S_{A,A} = \eta_{B,B}/D & S_{A,B} = -\eta_{B,A}/D \\ S_{B,A} = -\eta_{A,B}/D & S_{B,B} = \eta_{A,A}/D \end{bmatrix}, \quad (29)$$

grouping the chemical potential derivatives of the *grand*-potential

$$\Omega^+(\boldsymbol{\mu}_R^{+}) = E^+(\boldsymbol{N}_R) - \boldsymbol{\mu}_R^{+}\boldsymbol{N}_R.$$

It further generates the associated fragment and global response descriptors. For example, the softnesses of the bonded (embedded) subsystems in $R^* = (A^*¦B^*)$,

$$S_A^{R} = (\eta_{B,B} - \eta_{A,B})/D \equiv \eta_B^{R}/D,\ S_B^{R} = (\eta_{A,A} - \eta_{A,B})/D \equiv \eta_A^{R}/D, \quad (30)$$

generate the additive contributions to the global softness S_R of the whole R, the inverse of the global hardness η_R,

$$S_R = S_A^{R} + S_B^{R} = (\eta_A^{R} + \eta_B^{R})/D = \eta_R^{CT}/D = \eta_R^{-1}, \quad (31)$$

and the condensed FF indices of reactants:

$$f_A^{R} = \partial N_A/\partial N = S_A^{R}/S_R = \eta_B^{R}/\eta_R^{CT}$$

$$\text{and } f_B^{R} = \partial N_B/\partial N = S_B^{R}/S_R = \eta_A^{R}/\eta_R^{CT}. \quad (32)$$

Therefore, the resultant hardness of R as a whole can be directly expressed in terms of elements of the condensed hardness matrix in reactant resolution:

$$\eta_R = 1/S_R = D/\eta_R^{CT} = (\eta_{A,A}\eta_{B,B} - \eta_{A,B}\eta_{B,A})/(\eta_{A,A} + \eta_{B,B} - 2\eta_{A,B}). \quad (33)$$

The *fractional* populations of subsystems, and the average numbers of electrons on molecular fragments, require an ensemble description [21]. Indeed, the *external* inflow or outflow of electrons must involve a *macroscopic* electron reservoir, while in the *internal* exchanges in R one substrate acts as a *microscopic* "reservoir" to its reaction partner [16]. Contrary to the external *discontinuity* of the chemical potential in a molecular reactive system coupled to the *external* reservoir (Figure 1*a*) [20], the *in situ* electronegativity difference, which drives electron flows between the microscopic (externally closed) reactants, represents the *continuous* function of the fractional amount of CT: $E_R = E(N_{CT})$ [16]. This validates Mulliken's [19] parabolic interpolation and confirms it as a genuine energy function in an *internal* ensemble description.

In the ensemble approach to R^+ one refers to the *externally* open but *mutually* closed (chemically nonbonded) reactants in the composite macroscopic system $M^+ \equiv (R_A¦A^+|B^+¦R_B)$ involving separate electron reservoirs for each polarized substrate. The equilibrium shifts in subsystem populations, $\Delta\boldsymbol{N}_R^{+} = \{N_\alpha\}$, then respond to displacements in the reservoir chemical potentials $\Delta\boldsymbol{\mu}_R^{+} = \{\Delta\mu_\alpha\}$:

$$\Delta\boldsymbol{N}_R^{+} = \Delta\boldsymbol{\mu}_R^{+}\boldsymbol{\sigma}_R^{+} \text{ or } \boldsymbol{\mu}_R^{+} = \Delta\boldsymbol{N}_R^{+}\boldsymbol{\eta}_R^{+}. \quad (34)$$

The hardness $(\boldsymbol{\eta}_R^{+})$ and softness $(\boldsymbol{\sigma}_R^{+})$ matrices thus relate the equilibrium "displacements" in the reservoir chemical potentials, equal to the corresponding descriptors of

Citation: Nalewajski RF (2024) On population-space description of chemical reactivity. Open Journal of Chemistry 10(1): 047-057.
DOI: https://dx.doi.org/10.17352/ojc.000039

reactants, with the conjugate "responses" in fragment electron populations.

The DA system R(x) = $A^R(x)$ — $B^R(x)$, where x measures the current amount of the B→A CT, can be also viewed as a prototype of the bond-formation reaction between the initially *non*-bonded (polarized) reactants (Figure 1*c*):

$$(A^+|B^+) \rightarrow (A^*|B^*) \rightarrow (A^*\,\vdots\,B^*). \qquad (35)$$

The energy profile of this CT reaction is then derived from the resultant expression for the energy [see Eqs. (12) and (14b)]:

$$\Delta E(x) = \mu_R^{CT} x + ½\, \eta_R^{CT} x^2 = (\mu_A x + ½\eta_A^R x^2) + (-\mu_B x + ½\eta_B^R x^2) \equiv E_A^R(x) + E_B^R(x)$$

$$= [(\mu_A x + ½\eta_{A,A} x^2) + (-\mu_B x + ½\eta_{B,B} x^2)] - 2\eta_{A,B} x^2 \equiv [E_A(x) + E_B(x)] + E_{AB}(x). \qquad (36)$$

It is seen to combine contributions due to the *embedded* reactants in R: the "base-activation" curve $E_B^R(x)$ and the "acid-stabilization" function $E_A^R(x)$, with the "transition state" (TS) complex $R^‡ = (A^*|B^*)$ for $x^‡ = N_{CT}$ composed of the *closed* (nonbonded) equilibrium reactants $\{\alpha^*\}$, simultaneously population-activated. Sitting next to the *zero*-energy at the initial polarized complex for x = 0, $E(A^+|B^+) \equiv 0$, then identifies the reaction energy as that corresponding to the bonded, mutually-open reactants (Figure 1*a*):

$$E_r = E(A^*\,\vdots\,B^*) = E_{CT}. \qquad (37)$$

For a finite x, the *in situ* energy of CT complex has been alternatively partitioned in Eq. (36) into the *uncoupled*-reactant contributions $\{E_\alpha(x) > 0\}$ describing the $\{\alpha^+ \rightarrow \alpha(x)\}$ transitions, and the interaction energy:

$$E_{AB}(x) = -\,2\eta_{A,B}\, x^2 < 0. \qquad (38)$$

The latter stabilizes the reactive complex since the coupling hardness reflects the Coulomb repulsion between electrons on both fragments: $\eta_{A,B} \approx \gamma_{A,B} > 0$.

The typical energy profile for this *bond*-formation process (Figure 1*c*) can be viewed as consisting of the base-*activation* segment $E_B^R(x)$, for $0 \le x \le N_{CT}$, and the acid-*stabilization* part $E_A^R(x)$, for $N_{CT} \le x \le 2N_{CT}$, with the activation energy at the intersection point $x^‡ = N_{CT}$:

$$E_A^R(x^‡) = E_B^R(x^‡) \equiv E_a > 0. \qquad (39)$$

Alternatively, these two segments can be juxtaposed along a *common* CT-progress variable $y \in (0, N_{CT})$ measuring the current amount of the B→A CT (Figure 1*d*) [10-12]. The intersection $y^‡$ of the energy plots $E_B^R(y)$ and $E_A^R(y)$,

$$E_A^R(y^‡) = E_B^R(y^‡) \equiv E_a, \qquad (40)$$

then determines yet another representative position $y^‡ \equiv N_{CT}$ and activation energy E_a for the isoelectronic CT in AB systems. This representation facilitates a discussion of "dynamical" aspects of the Hard(H)–Soft(S) Acids(A) and Bases(B) (HSAB) principle of chemistry (Figure 1*e*) [7,10-12,22-26]. One recalls, that the *opposite*-hardness combinations H–S and S–H have been identified as producing relatively unstable complexes, with the *comparable*-hardness compounds H–H and S–S acquiring their relative stability due to stronger *inter*-substrate chemical bonds: covalent in S–S complex [7] and ionic in H–H compound [23]. Indeed, the largest values of CT-amount should characterize the *covalent*, S-S structure, the mixed-hardness species are predicted to exhibit moderate values of N_{CT}, while its lowest value can be expected in the *ionic*, H-H structures. A reference to Figure 1*e* shows that all these hardness combinations generate a cluster of similar energies $\{E_a\}$ and corresponding CT measures $\{N_{CT}\}$, predicting an "early" position of a "low" activation barrier. Specific orderings in these predictions should depend strongly on the actual combinations of reactant harnesses (compare [10,11,12]).

Atomic resolution of electronic reorganizations and intersecting-state model

For some interpretations in chemistry the preceding "condensed" perspective, in which reactants are viewed as whole units, may require a more detailed resolution, e.g., in terms of the (bonded) constituent AIM, the system occupied MO or the AO basis functions of molecular calculations.

Consider the illustrative case of *atomic* approach to the DA reactive system R, with the row vectors $\boldsymbol{N}_A = \{N_a\}$ and $\boldsymbol{N}_B = \{N_b\}$ now grouping the average AIM populations in both substrates, $\sum_a N_a = N_A$ and $\sum_b N_b = N_B$, for the fixed external potential $v(\boldsymbol{r}) = v_A(\boldsymbol{r}) + v_B(\boldsymbol{r})$ due to the rigid molecular geometry. They combine into the overall population (row) vector in atomic resolution, $\boldsymbol{N}^R = (\boldsymbol{N}_A, \boldsymbol{N}_B)$, with the system electronic energy being now regarded as its function: $E^R(\boldsymbol{N}^R) = E^R(\{\boldsymbol{N}_\alpha\})$. This selection of electronic variables in turn determines the associated differential descriptors: the *row* vector of atomic chemical potentials,

$$\boldsymbol{u}^R = \partial E^R/\partial \boldsymbol{N}^R = (\boldsymbol{u}_A, \boldsymbol{u}_B) = \{\boldsymbol{u}_\alpha = \partial E(\boldsymbol{N}^R)/\partial \boldsymbol{N}_\alpha\}, \qquad (41)$$

and the *square* hardness matrix in atomic resolution:

$$\mathbf{h}^R = \partial^2 E^R/\partial \boldsymbol{N}^R\, \partial \boldsymbol{N}^R = \partial \boldsymbol{u}^R/\partial \boldsymbol{N} = \{\partial \boldsymbol{u}/\partial \boldsymbol{N}_\alpha \equiv \mathbf{h}_{\alpha,\beta} = \mathbf{h}_{\beta,}^{\,T} \equiv [\partial \boldsymbol{u}_\alpha/\partial \boldsymbol{N}_\beta]^T\}. \qquad (42)$$

The latter ultimately determines the AIM softness descriptors:

Citation: Nalewajski RF (2024) On population-space description of chemical reactivity. Open Journal of Chemistry 10(1): 047-057. DOI: https://dx.doi.org/10.17352/ojc.000039

$$\mathbf{s}^{\mathrm{R}} = (\mathbf{h}^{\mathrm{R}})^{-1} = \partial \boldsymbol{N}^{\mathrm{R}}/\partial \boldsymbol{u}^{\mathrm{R}} = \{\mathbf{s}_{\beta,\alpha} = \partial \boldsymbol{N}_{\alpha}/\partial \boldsymbol{u}_{\beta}\}. \quad (43)$$

This softness matrix now transforms the resolution chemical-potential displacements u^{R} into the conjugate populational responses $\Delta \boldsymbol{N}^{\mathrm{R}}$:

$$\Delta \boldsymbol{N}^{\mathrm{R}} = \Delta \boldsymbol{u}^{\mathrm{R}}\, \mathbf{s}^{\mathrm{R}} \text{ or } \Delta \boldsymbol{u}^{\mathrm{R}} = \Delta \boldsymbol{N}^{\mathrm{R}}\, \mathbf{h}^{\mathrm{R}}. \quad (44)$$

The *second*-order change in electronic energy due to populational displacements ΔN^{R} of AIM then reads:

$$\Delta E(\Delta \boldsymbol{N}^{\mathrm{R}}) = \Delta \boldsymbol{N}^{\mathrm{R}}\, \boldsymbol{u}^{\mathrm{R,T}} + \tfrac{1}{2}\, \Delta \boldsymbol{N}^{\mathrm{R}}\, \mathbf{h}^{\mathrm{R}}\, \Delta \boldsymbol{N}^{\mathrm{R,T}} \equiv \Delta E^{(1)}(\Delta \boldsymbol{N}^{\mathrm{R}}) + \Delta E^{(2)}(\Delta \boldsymbol{N}^{\mathrm{R}}). \quad (45)$$

Its quadratic term

$$\Delta E^{(2)}(\Delta \boldsymbol{N}^{\mathrm{R}}) = \tfrac{1}{2} \textstyle\sum_{\alpha}\sum_{\beta} \Delta \boldsymbol{N}_{\alpha}\, \mathbf{h}_{\alpha,\beta}\, \Delta \boldsymbol{N}_{\beta}^{\mathrm{T}} \equiv \sum_{\alpha}\sum_{\beta} \Delta E^{(2)}(\alpha,\beta), \quad (46)$$

defines in atomic resolution the energy paraboloid of the CT reactive system. It contains the (diagonal) *intra*-reactant surfaces (Figure 2),

$$E_{\alpha}^{+}(\Delta \boldsymbol{N}_{\alpha}) \equiv \Delta E^{(2)}(\alpha,\alpha) = \tfrac{1}{2}\, \Delta \boldsymbol{N}_{\alpha}\, \mathbf{h}_{\alpha,\alpha'}\, \Delta \boldsymbol{N}_{\alpha'}^{\mathrm{T}} = \tfrac{1}{2} \textstyle\sum_{a}\sum_{a'} N_{a}\, h_{a,a'}\, \Delta N_{a'},\ \alpha = \mathrm{A, B}; \quad (47a)$$

and the (*off*-diagonal) interaction contribution for $\alpha \neq \beta$

$$\Delta E^{(2)}(\alpha,\beta) + \Delta E^{(2)}(\beta,\alpha) = \textstyle\sum_{a\in\alpha}\sum_{b\in\beta} \Delta N_{a}\, h_{a,b}\, \Delta N_{b}. \quad (47b)$$

These canonical descriptors of AIM in R = AB can be also combined into the *global* reactant properties of the preceding section, and ultimately into those describing R as a whole. This is effected by weighting them into the average descriptors using the appropriate set of (atomic)

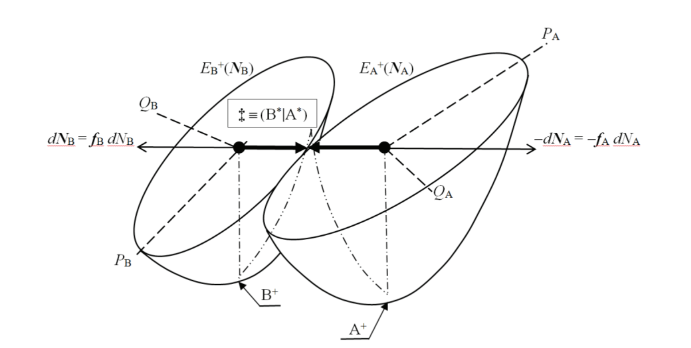

Figure 2: Population activation (A^+B^+) → ($A^*|B^*$) of the initially polarized (mutually-*closed*) reactants {α^+}, each exhibiting two internal (populational) degrees-of-freedom, $\boldsymbol{N}_A = \{N_a, N_{a'}\}$ and $\boldsymbol{N}_B = \{N_b, N_{b'}\}$. This displacement of the average populations in subsystems, $N_A = N_a + N_{a'}$ and $N_B = N_b + N_{b'}$, respectively, is effected in the externally *open* composite system ($R_A¦A^+|B^+|R_B$), which involves a *separate* reservoir for each subsystem. In the *isoelectronic* CT process, when $dN_A + dN_B = 0$, the displaced substrate populations, $dN_A = N_{CT}$ and $dN_B = -N_{CT}$, correspond to a common direction of the reactant internal FF {$\boldsymbol{f}_a = \partial N_a/\partial N_\alpha$}. This convention mutually orients both the AIM population spaces {$\boldsymbol{N}_\alpha$} of subsystems and their energy paraboloids {$E_\alpha^+(\boldsymbol{N}_\alpha) = \tfrac{1}{2}\sum_{i\in\alpha}\sum_{j\in\alpha} dN_i^{\alpha}\, \eta_{i,j}^{\alpha}\, dN_j^{\alpha} = \tfrac{1}{2}\,[h_P^{\alpha}\,(dN_P^{\alpha})^2 + h_Q^{\alpha}\,(dN_Q^{\alpha})^2]$}, determined by the (diagonal) reactant blocks $\mathbf{h}_{\alpha,\alpha}$ of the system overall hardness matrix in atomic resolution: $\mathbf{h}^{\mathrm{R}} = \{\mathbf{h}_{\alpha,\beta}\}$; here P_α and Q_α respectively denote the "polarization" and "charge-transfer" (CT) *normal* modes of reactant α^+, polarized in presence of its molecular partner.

FF indices:

$$\mathbf{G}^{\mathrm{R}} = \partial \boldsymbol{N}^{\mathrm{R}}/\partial \boldsymbol{N}_{\mathrm{R}} = \{\boldsymbol{g}_{\alpha} = \partial \boldsymbol{N}^{\mathrm{R}}/\partial N_{\alpha}\}. \quad (48)$$

The *chain*-rule transformation of derivatives provides the required combination rules:

$$\mu_{\alpha} = \partial E^{+}(\boldsymbol{N}_{\mathrm{R}})/\partial N_{\alpha} = \partial E^{\mathrm{R}}(\boldsymbol{N}^{\mathrm{R}})/\partial N_{\alpha} = (\partial \boldsymbol{N}^{\mathrm{R}}/\partial N_{\alpha})\, (\partial E^{\mathrm{R}}/\partial \boldsymbol{N}^{\mathrm{R}}) \equiv \boldsymbol{g}_{\alpha}\, \boldsymbol{u}^{\mathrm{R,T}}$$

$$= \textstyle\sum_{\beta} (\partial \boldsymbol{N}_{\beta}/\partial N_{\alpha})\, (\partial E^{\mathrm{R}}/\partial \boldsymbol{N}_{\beta}) \equiv \sum_{\beta} G_{\alpha,\beta}\, \boldsymbol{u}_{\beta}^{\mathrm{T}} \text{ or } \boldsymbol{\mu}_{\mathrm{R}}^{+} = \mathbf{G}^{\mathrm{R}}\, \boldsymbol{u}^{\mathrm{R,T}}; \quad (49)$$

$$\eta_{\alpha,\beta} = \partial^2 E^{+}(\boldsymbol{N}_{\mathrm{R}})/\partial N_{\alpha}\partial N_{\beta} = = \partial^2 E^{\mathrm{R}}(\boldsymbol{N}^{\mathrm{R}})/\partial N_{\alpha}\partial N_{\beta}$$

$$= (\partial \boldsymbol{N}^{\mathrm{R}}/\partial N_{\alpha})\, (\partial^2 E^{\mathrm{R}}/\partial \boldsymbol{N}^{\mathrm{R}}\partial \boldsymbol{N}^{\mathrm{R}})\, (\partial \boldsymbol{N}^{\mathrm{R}}/\partial N_{\beta}) = \boldsymbol{g}_{\alpha}\, \mathbf{h}^{\mathrm{R}}\, \boldsymbol{g}_{\beta}^{\mathrm{T}}$$

$$= \textstyle\sum_{\gamma}\sum_{\delta} (\partial \boldsymbol{N}_{\gamma}/\partial N_{\alpha})\, (\partial^2 E^{\mathrm{R}}/\partial \boldsymbol{N}_{\gamma}\, \partial \boldsymbol{N}_{\delta})\, (\partial \boldsymbol{N}_{\delta}/\partial N_{\beta}) \equiv \sum_{\gamma}\sum_{\delta} \boldsymbol{G}_{\alpha,\gamma}\, \mathbf{h}_{\gamma,\delta}\, \boldsymbol{G}_{\delta,\alpha}^{\mathrm{T}} \text{ or}$$

$$\boldsymbol{\eta}_{\mathrm{R}}^{+} = \mathbf{G}^{\mathrm{R}}\, \mathbf{h}^{\mathrm{R}}\, \mathbf{G}^{\mathrm{R,T}}. \quad (50)$$

Here, the combined matrix of *internal* FF descriptors of constituent atoms in both reactants reads

$$\begin{bmatrix} \boldsymbol{G}_{\mathrm{A,A}} = \partial \boldsymbol{N}_{\mathrm{A}}/\partial N_{\mathrm{A}},\ \boldsymbol{G}_{\mathrm{A,B}} = \partial \boldsymbol{N}_{\mathrm{B}}/\partial N_{\mathrm{A}} \\ \boldsymbol{G}_{\mathrm{B,A}} = \partial \boldsymbol{N}_{\mathrm{A}}/\partial N_{\mathrm{B}},\ \boldsymbol{G}_{\mathrm{B,B}} = \partial \boldsymbol{N}_{\mathrm{B}}/\partial N_{\mathrm{B}} \end{bmatrix} \quad (51)$$

and the *external* FF indices $\boldsymbol{F}^{\mathrm{R}} = \partial \boldsymbol{N}^{\mathrm{R}}/\partial N_{\mathrm{R}}$ group the populational responses of AIM to an inflow or outflow dN_{R} of electrons to/from R as a whole:

$$\boldsymbol{F}^{\mathrm{R}} = \partial \boldsymbol{N}^{\mathrm{R}}/\partial N_{\mathrm{R}} = (\boldsymbol{F}_{\mathrm{A}}^{\ \mathrm{R}} = \partial \boldsymbol{N}_{\mathrm{A}}/N_{\mathrm{R}},\ \boldsymbol{F}_{\mathrm{B}}^{\ \mathrm{R}} = \partial \boldsymbol{N}_{\mathrm{B}}/\partial N_{\mathrm{R}}). \quad (52)$$

The diagonal blocks in $\mathbf{G}^{\mathrm{R}}$ define the *internal* FF of AIM in each separate reactant (Figures 2,3):

$$\boldsymbol{G}_{\mathrm{A,A}} = \partial \boldsymbol{N}_{\mathrm{A}}/\partial N_{\mathrm{A}} \equiv \boldsymbol{f}_{\mathrm{A}} = \{\boldsymbol{f}_{a} = \partial N_{a}/\partial N_{\mathrm{A}}\} \text{ and}$$

$$\boldsymbol{G}_{\mathrm{B,B}} = \partial \boldsymbol{N}_{\mathrm{B}}/\partial N_{\mathrm{B}} \equiv \boldsymbol{f}_{\mathrm{B}} = \{f_{b} = \partial N_{b}/\partial N_{\mathrm{B}}\}. \quad (53)$$

The resultant chemical potential and hardness of the whole reactive complex are given by the appropriate FF-weighted, external averages of AIM descriptors:

$$\mu_{\mathrm{R}} = \partial E^{\mathrm{R}}/\partial N_{\mathrm{R}} = (\partial \boldsymbol{N}^{\mathrm{R}}/N_{\mathrm{R}})\, (\partial E^{\mathrm{R}}/\partial \boldsymbol{N}^{\mathrm{R}}) = \boldsymbol{F}^{\mathrm{R}}\, \boldsymbol{u}^{\mathrm{R,T}}$$

$$= \textstyle\sum_{\alpha} (\partial \boldsymbol{N}_{\alpha}/\partial N_{\mathrm{R}})\, (\partial E^{\mathrm{R}}/\partial \boldsymbol{N}_{\alpha}) = \sum_{\alpha} \boldsymbol{F}_{\alpha}^{\ \mathrm{R}}\, \boldsymbol{u}_{\alpha}^{\ \mathrm{T}}, \quad (54)$$

$$\eta_{\mathrm{R}} = \partial^2 E_{\mathrm{R}}/\partial N_{\mathrm{R}}^{\ 2} = (\partial \boldsymbol{N}^{\mathrm{R}}/\partial N_{\mathrm{R}})\, (\partial^2 E^{\mathrm{R}}/\partial \boldsymbol{N}^{\mathrm{R}}\partial \boldsymbol{N}^{\mathrm{R}})\, (\partial \boldsymbol{N}^{\mathrm{R}}/\partial N_{\mathrm{R}}) = \boldsymbol{F}^{\mathrm{R}}\, \mathbf{h}^{\mathrm{R}}\, \boldsymbol{F}^{\mathrm{R,T}}$$

$$= \textstyle\sum_{\alpha}\sum_{\beta} (\partial \boldsymbol{N}_{\alpha}/\partial N_{\mathrm{R}})\, (\partial^2 E^{\mathrm{R}}/\partial \boldsymbol{N}_{\alpha}\, \partial \boldsymbol{N}_{\beta})\, (\partial \boldsymbol{N}_{\beta}/\partial N_{\mathrm{R}}) = \sum_{\alpha}\sum_{\beta} \boldsymbol{F}_{\alpha}^{\ \mathrm{R}}\, \mathbf{h}_{\alpha,\beta}\, \boldsymbol{F}_{\beta}^{\ \mathrm{R,T}}. \quad (55)$$

The atomic resolution of electronic structure offers chemically interesting details of molecular rearrangements in chemical reactions. They cover descriptors of both the "internal", N-restricted process of the bond-formation

Citation: Nalewajski RF (2024) On population-space description of chemical reactivity. Open Journal of Chemistry 10(1): 047-057.
DOI: https://dx.doi.org/10.17352/ojc.000039

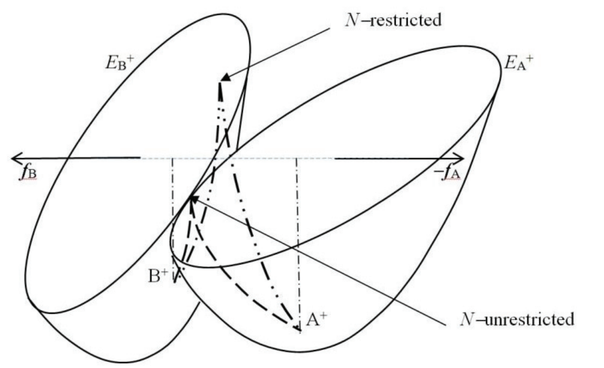

Figure 3: Moderating effect of the reactant *external*-opening in the composite system $M^+ \equiv (R_A{\mid}A^+{\mid}B^+{\mid}R_B)$ upon the activation energy of CT systems: $E_a^{\text{restricted}} > E_a^{\text{unrestricted}}$.

between reactants and the "external", *N*-unrestricted effects, due to the intervention of an electronic reservoir. A reference to Figure 3 indeed suggests, that such an "opening" of the reactive system in the *N*-unrestricted CT should lower the required activation energy (see also [10-12]).

When combining reactant paraboloids in ISM one ultimately encounters the problem of the unique mutual orientation of the AIM population spaces in both reactants. The natural choice is dictated by the requirement that the reactant FF vectors of Eq. (53) are collinear in the isoelectronic, *N*-restricted CT processes in DA systems. Indeed, electrons removed from the *basic* subsystem, most efficiently along the $\boldsymbol{f}_B$ direction, are subsequently donated to the *acidic* subsystem, most effectively along the $\boldsymbol{f}_A$ vector. This convention is adopted in Figures 2,3.

The *N*-unrestricted mechanism deviates from this collinearity (Figure 3). It can be realized in catalytic systems, where the surface active sites provide electron reservoirs for chemisorbed reactants. A reference to Figure 3 also shows that this external opening of reactants may have a moderating effect on their activation in CT processes. The "softening" influence of the system environment should thus constitute an important factor in the catalytic activity of heterogeneous systems.

The Mulliken-type formulas [4,10,16,19],

$$u_k \approx -½\,[I_k + A_k] \equiv u_k^{(M)},\; h_{k,k} \approx I_k - A_k \equiv h_{k,k}^{(M)},\; h_{k,l} \approx ½[h_{k,k} + h_{l,l}] \equiv h_{k,l}^{(M)}, \qquad (56)$$

approximate the canonical AIM data of Eqs. (41) and (42). The *off*-diagonal hardnesses in $\mathbf{h}^R = \{h_{k,l} = \partial^2 E^R/\partial N_k\,\partial N_l = \partial u_l/\partial N_k\}$, can be then "scaled" geometrically,

$$h_{k,l} \approx h_{k,l}^{(M)}\, S_{k,l}(R_{k,l}), \qquad (57)$$

where $S_{k,l}$ stands for the overlap integral $S_{k,l} = \langle s_k|s_l\rangle$ between the representative *s*-type orbitals in the valence shells of atoms *k* and *l*. This representation separates the "property" descriptor $h_{k,l}^{(M)}$ from its geometrical factor $S_{k,l}(R_{k,l})$, depending on the *inter*-atomic distance $R_{k,l}$. It correctly reproduces the diagonal *atomic* descriptor, for $k = l$ and hence $S_{k,k}(R_{k,k}{=}0) = 1$, and predicts the vanishing population coupling at large distances: $S_{k,l}(R_{k,l} \to \infty) = 0$. This estimate of the coupling hardness also satisfies the Maxwell *cross*-differentiation identity: $h_{k,l} = h_{l,k}$. Such *finite*-difference data can be ultimately transformed into the reactant descriptors of Eqs. (49) and (50).

Alternatively, the interpolations of the *valence*-shell electron-repulsion integrals, familiar from the *semi*-empirical LCAO MO theories, e.g., the Mataga-Nishimoto or Ohno formulas, can be used to approximate the hardness tensor in atomic resolution [10,27].

The *finite*-difference measures of the fragment chemical potentials $\{\mu_\alpha^{(M)} = (I_\alpha + A_\alpha)/2\}$ and hardnesses $\{\eta_\alpha^{(M)} = I_\alpha - A_\alpha\}$ of *mono*-atomic reactants, A = *k* and B = *l*, generate the following *in situ* descriptors for the "positive" B→A CT, consistent with chemical functions of both substrates in reactive complex (Figure 1*a*):

$$\mu_R^{CT} \approx \mu_A^{(M)} - \mu_B^{(M)} = ½\,[(I_B + \mathrm{a}\,A_B) - (I_A + A_A)]$$

$$= ½\,[(I_B - A_A) - (I_A - A_B)] = ½\,[\mu_{CT}^{(+)} - \mu_{CT}^{(-)}] < 0, \qquad (58)$$

$$\eta_R^{CT} \approx \eta_{A,A}^{(M)} + {}_{B,B}^{(M)} - 2\eta_{A,B}^{(M)}$$

$$= [(I_B - A_A) + (I_A - A_B)]\,(1 - S_{A,B}) = [\mu_{CT}^{(+)} + \mu_{CT}^{(-)}]\,(1 - S_{A,B}) > 0, \qquad (59)$$

$$N_R^{CT} = -\,\mu_R^{CT}/\eta_R^{CT} = [\mu_{CT}^{(-)} - \mu_{CT}^{(+)}]/\{2[\mu_{CT}^{(+)} + \mu_{CT}^{(-)}]\,(1 - S_{A,B})\} > 0, \qquad (60)$$

$$E_{CT} = -\,½\,(\mu_R^{CT})^2/\eta_R^{CT} = -\,½\,[\mu_{CT}^{(+)} - \mu_{CT}^{(-)}]^2/\{(1 - S_{A,B})\,[{}_{CT}^{(+)} + \mu_{CT}^{(-)}]\}. \qquad (61)$$

These expressions in terms of the *biased* chemical potentials for the reverse directions of CT indicate that an increasing overlap between reactants effectively softens the reactive system, thus facilitating a larger CT amount and greater stabilization energy.

Composite structures involving acid–base complexes

This populational perspective on the molecular electronic structure may also involve larger molecular fragments, e.g., the active parts of the acceptor and donor

Citation: Nalewajski RF (2024) On population-space description of chemical reactivity. Open Journal of Chemistry 10(1): 047-057.
DOI: https://dx.doi.org/10.17352/ojc.000039

substrates. Let us symbolically separate the geometrically accessible acidic (a) and basic (b) sites in reactants $\alpha \in$ (A, B) from their immaterial remainders:

$$A = (a_A\!\!\mid\!\ldots\!\mid\!b_A) \equiv (a_A\!\mid\!b_A) \text{ and } B = (a_B\!\mid\!\ldots\!\mid\!b_B) \equiv (a_B\!\mid\!b_B).$$

There are two alternative mutual arrangements of such subsystems in the TS complex: the *complementary* (c) structure R_c (Figure 4), in which the a-site of one reactant faces the b-site of the other substrate, and the regional-HSAB, *parallel* (p) structure $R_p = R_{HSAB}$, when mutually coordinating sites of both reactants are of the *like*-hardness character [28-30]:

$$R_c \equiv \begin{bmatrix} a_A - b_B \\ b_A - a_B \end{bmatrix} \text{ and } R_{HSAB} \equiv \begin{bmatrix} a_A - a_B \\ b_A - b_B \end{bmatrix} \equiv R_p. \qquad (62)$$

The acidic (acceptor) site is relatively harder, i.e., less sensitive to an external perturbation, thus exhibiting lower values of the fragment FF index or the associated chemical-softness descriptor, while the basic (donor) fragment is more polarizable, as indeed reflected by its higher response properties. The acidic part in X exerts an electron-*accepting* (stabilizing) influence on the neighboring fragment of the other reactant Y, while the basic site of X produces an electron-*donor* (destabilizing) effect on the coordinated region of Y in its vicinity. The purely electrostatic, "ionic" interactions a_A—b_B and a_B—b_A then allow one to predict R_c as the expected preferred structure, while the "covalent" interactions a_A—a_B and b_B—b_A of the HSAB principle point towards R_p as the most stable system. Numerical calculations [28] confirm that *complementary* interactions of Figure 4, between the electron-*rich* (basic) fragment of one reactant and the electron-*deficient* (acidic) fragment of another substrate, indeed establish the most stable TS complex.

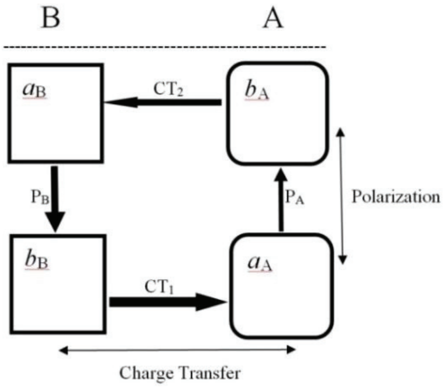

Figure 4: The elementary CT $\{b_X \to a_Y\}$ and polarizational (P) $\{a_X \to b_X\}$ flows of electrons involving acidic $A \equiv (a_A\!\mid\!b_A)$ and basic $B \equiv (a_B\!\mid\!b_B)$ reactants in the *complementary* arrangement R_c of their acidic (a) and basic (b) sites in the reactive complex. These shifts are seen to produce the concerted ("circular") pattern of electronic fluxes in the final, equilibrium reactive system $R_c^* = (A^*\!\mid\!B^*) = (a_A\!\mid\!b_A\!\mid\!a_B\!\mid\!b_B)$, when all fragments are free to exchange electrons.

This relative stability of R_c reflects an electrostatic dominance in A—B interactions: a (repulsive) basic fragment of one reactant indeed prefers to face an (attractive) acidic part of the reaction partner. The displacements in reactant external potentials due to the presence of the other substrate trigger the induced *polarization* flows $\{P_X\}$, which restore the initially displaced *intra*-substrate equilibria of isolated species. The *inter*-reactant CT displacements, after the hypothetical opening of the initially closed, polarized reactants, can be directly inferred from the Electronegativity Equalization (EE) principle [31,32]. The combined networks of P and CT displacements between the TS active sites,

$$R_c: \begin{tikzcd} a_B \arrow[d] & b_A \arrow[l] \\ b_B \arrow[r] & a_A \arrow[u] \end{tikzcd} \quad \text{and} \quad R_p: \begin{tikzcd} a_B \arrow[r] & a_A \\ b_B \arrow[u] \arrow[r] & b_A \arrow[u] \end{tikzcd},$$

then reveal different patterns of probability fluxes in these two reactive complexes: the "concerted" pattern in R_c and the "disconcerted" flow system in R_p [29,30]. They imply the least population displacements (activation) of both reactants in the former and more exaggerated charge displacements on the crucial a_A and b_B sites of the latter. Indeed, in R_c one observes the flow-through behavior on all four active sites, with small *net* changes in electron populations on all these fragments, while the charge reconstruction in R_p can be regarded as a transfer of electrons from b_B to a_A through the remaining (intermediate) sites a_B and b_A. The concerted flows in R_c, which preclude an exaggerated charge depletion or accumulation, thus correspond to the least-displaced electron populations on all four reaction sites. This activation (promotion) perspective provides an additional physical explanation of the complementary preference.

Compared to the isolated species A^0 and B^0, the *primary* coordination B→A in equilibrium DA system ultimately produces an electron-*deficient* basic substrate $B^{+} \equiv B^{(+)}$ and an *excess* electron population on its acidic partner $A^{-\delta} \equiv A^{(-)}$:

$$B \to A \equiv [A^*\!\mid\!B^*] = A^{(-)}\text{—}B^{(+)} \equiv M. \qquad (63)$$

Each of the "displaced" reactants then acquires partially "opposite" external character: $A^{(-)}$ site exhibits an increased tendency to *donate* electrons to its environment, while $B^{(+)}$ becomes an effective electron-*acceptor* site: $a_M = B^{(+)}$ and $b_M = A^{(-)}$. In external interactions between "monomers" $\{M_i\}$, the *bonded* A^0 part of one unit thus represents an accessible "basic" site for interactions with another AB complex, while the *bonded* $B^{(+)}$ fragment stands for an available "acidic" site. Such *secondary*, "response" actions may influence how such units ("monomers") combine into larger, *supra*-molecular structures ("polymers").

Citation: Nalewajski RF (2024) On population-space description of chemical reactivity. Open Journal of Chemistry 10(1): 047-057.
DOI: https://dx.doi.org/10.17352/ojc.000039

In the spirit of the *maximum complementarity* [19], the preferred structure of the dimer $D_c = M_2$ then involves the following pattern of "secondary" coordinations between bonded reactants of different monomers:

$$D_c = \begin{array}{ccccc} A^{(-)} & — & B^{(+)} & & M_1 \\ \downarrow & & \uparrow & \equiv & \updownarrow \\ B^{(+)} & — & A^{(-)} & & M_2 \end{array}$$

For the trimer $T_c = M_3$ one similarly conjectures the following two alternative structures:

Linear (L),

$$T_c(L) = \begin{array}{ccccc} A^{(-)} & — & B^{(+)} & & M_1 \\ \downarrow & & \uparrow & & \updownarrow \\ B^{(+)} & — & A^{(-)} & \equiv & M_2 \\ \uparrow & & \downarrow & & \updownarrow \\ A^{(-)} & — & B^{(+)} & & M_3 \end{array}$$

and *Cyclic* (C):

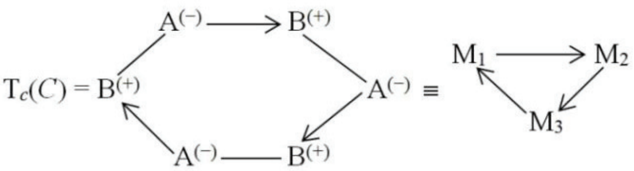

In all these associations of the (bonded) Acid-Base complexes the "primary" (internal) coordinations $A \rightarrow B = A^{(-)}—B^{(+)}$ (in monomers) and the "secondary" (external) actions $M_i \rightarrow M_j$ (between monomers), are seen to enhance each other.

Conclusion

Electron redistributions in chemical processes, and the associated changes of electronic populations on molecules and their active parts ultimately determine the structural patterns and reactivity trends of reactive systems. Different aspects of a "chemical" behavior may require specific reactivity criteria, all dependent on the current distribution of electrons in molecular systems. They may correspond to both the externally *closed* and -*open* conditions, each calling for specific descriptors of interacting substrates and displacements in the system's electronic energy.

In this work, we have explored such populational characteristics of CT processes in A(acceptor)—B(donor) systems, in both the substrate and AIM resolution levels. The simple models of CT reactivity and ISM in AIM resolution have been reexamined, and the "biased" and "unbiased" measures of reactant chemical potentials and their differences driving N-restricted CT have been discussed. The implications of their *discontinuity* in the *macroscopic* ensemble and continuity in Mulliken's *internal* ensemble approach have also been stressed. The FF convention for uniting the AIM population spaces of reactants in ISM has been revisited and model implications for lower activation energies in catalytic systems have been reiterated. We have also tackled the combination rules for the condensed CT-reactivity criteria in terms of the corresponding AIM descriptors.

Typical reactivity concepts have been invoked at both the P and CT reaction stages. A qualitative discussion of the DA complexes and composite systems consisting of AB monomers has also been given. In AB interactions a dominance of the molecular *complementarity* over the *regional*-HSAB behavior has been emphasized and its implications for predicted $(AB)_n$ structures have been explored. It has been stressed, that the "primary" B→A coordination in donor-acceptor complexes "reverses" chemical characters of the acidic and basic reactants, thus having a profound influence on the stable patterns of the "secondary" associations of such AB monomers. In such "polymer" structures the internal and external coordinations enhance each other.

References

1. Hohenberg P, Kohn W. Inhomogeneous electron gas. Phys Rev. 1964; 136B:864-871.
2. Kohn W, Sham LJ. Self-consistent equations including exchange and correlation effects. Phys Rev. 1965; 140A:1133-1138.
3. Levy M. Universal variational functionals of electron densities, first-order density matrices, and natural spin-orbitals and solution of the v-representability problem. Proc Natl Acad Sci USA. 1979;76(12):6062-6065.
4. Parr RG, Yang W. Density-functional theory of atoms and molecules. New York: Oxford University Press; 1989.
5. Dreizler RM, Gross EKU. Density functional theory: an approach to the quantum many-body problem. Berlin: Springer; 1990.
6. Nalewajski RF, editor. Density functional theory I-IV: Topics in Current Chemistry 180-183. Heidelberg: Springer-Verlag; 1996.
7. Parr RG, Pearson RG. Absolute hardness: companion parameter to absolute electronegativity. J Am Chem Soc. 1983; 105(24):7512-7516.
8. Parr RG, Yang W. Density functional approach to the frontier-electron theory of chemical reactivity. J Am Chem Soc. 1984; 106(14):4049-4050.
9. Nalewajski RF, Korchowiec J, Michalak A. Reactivity criteria in charge sensitivity analysis. In: Nalewajski RF, editor. Density functional theory IV: Topics in Current Chemistry 183. 1996; 183:25-141.
10. Nalewajski RF, Korchowiec J. Charge sensitivity approach to electronic structure and chemical reactivity. Singapore: World Scientific; 1997.
11. Nalewajski RF. Sensitivity analysis of charge transfer systems: in situ quantities, intersecting-state model and its implications. Int J Quantum Chem. 1994; 49(5):675-703.
12. Nalewajski RF. Charge sensitivity analysis as diagnostic tool for predicting trends in chemical reactivity. In: Dreizler RM, Gross EKU, editors. Proceedings

Citation: Nalewajski RF (2024) On population-space description of chemical reactivity. Open Journal of Chemistry 10(1): 047-057.
DOI: https://dx.doi.org/10.17352/ojc.000039

of the NATO ASI on Density Functional Theory (Il Ciocco, 1993). New York: Plenum; 1995; 339-389.

13. Geerlings P, De Proft F, Langenaeker W. Conceptual density functional theory. Chem Rev. 2003 May;103(5):1793-873. doi: 10.1021/cr990029p. PMID: 12744694.

14. Chattaraj PK, editor. Chemical reactivity theory: a density functional view. Boca Raton: CRC Press; 2009.

15. Ghosh SK, Chattaraj PK, editors. Concepts and methods in modern theoretical chemistry: Electronic structure and chemical reactivity. Boca Raton: CRC Press; 2013.

16. Nalewajski RF. Chemical reactivity in quantum mechanics and information theory. Elsevier, New York; 2023.

17. Nalewajski RF. Information theory of molecular systems. Amsterdam: Elsevier; 2006.

18. Ciosłowski J, Mixon ST. Electronegativities in situ, bond hardnesses, and charge-transfer components of bond energies from the topological theory of atoms in molecules. J Am Chem Soc. 1993;115(3):1084-1088.

19. Mulliken RS. A new electronegativity scale: together with data on valence states and on ionization potentials and electron affinities. J Chem Phys. 1934; 2(11):782-793.

20. Perdew JP, Parr RG, Levy M, Balduz JL. Density functional theory for fractional particle number: derivative discontinuities of the energy. Phys Rev Lett. 1982; 49(23):1691-1694.

21. Gyftopoulos EP, Hatsopoulos GN. Quantum-thermodynamic definition of electronegativity. Proc Natl Acad Sci U S A. 1968 Jul;60(3):786-93. doi: 10.1073/pnas.60.3.786. PMID: 16591659; PMCID: PMC225120.

22. Pearson RG. Hard and soft acids and bases. Stroudsburg: Dowden, Hutchinson and Ross; 1973.

23. Nalewajski RF. Electrostatic effects in interactions between hard (soft) acids and bases. J Am Chem Soc. 1984; 106(4):944-945.

24. Chattaraj PK, Lee H, Parr RG. HSAB principle. J Am Chem Soc. 1991; 113(6):1855-1856.

25. Gazquez JL, Mendez F. The hard and soft acids and bases principle: an atoms-in-molecules viewpoint. J Phys Chem. 1994; 98(17):4591-4593.

26. Ayers PW. The physical basis of the hard/soft acid/base principle. Faraday Discuss. 2007; 135:161-190.

27. Nalewajski RF, Korchowiec J, Zhou Z. Molecular hardness and softness parameters and their use in chemistry. Int J Quantum Chem Symp. 1988; 22:349-366.

28. Chandra AK, Michalak A, Nguyen MT, Nalewajski RF. On regional matching of atomic softnesses in chemical reactions: two-reactant charge sensitivity study. J Phys Chem A. 1998; 102(48):10182-10188.

29. Nalewajski RF. Manifestations of the maximum complementarity principle for matching atomic softnesses in model chemisorption systems. Top Catal. 2000; 11:469-485.

30. Nalewajski RF. Understanding electronic structure and chemical reactivity: quantum-information perspective. In: Sousa S, editor. The application of quantum mechanics to the reactivity of molecules. Appl Sci. 2019;9:1262-1292.

31. Sanderson RT. An interpretation of bond lengths and a classification of bonds. Science. 1951; 114: 670-672.

32. Sanderson RT. Chemical bonds and bond energy. 2nd edn. Academic Press, New York. 1976.

Discover a bigger Impact and Visibility of your article publication with Peertechz Publications

Highlights

- Signatory publisher of ORCID
- Signatory Publisher of DORA (San Francisco Declaration on Research Assessment)
- Articles archived in worlds' renowned service providers such as Portico, CNKI, AGRIS, TDNet, Base (Bielefeld University Library), CrossRef, Scilit, J-Gate etc.
- Journals indexed in ICMJE, SHERPA/ROMEO, Google Scholar etc.
- OAI-PMH (Open Archives Initiative Protocol for Metadata Harvesting)
- Dedicated Editorial Board for every journal
- Accurate and rapid peer-review process
- Increased citations of published articles through promotions
- Reduced timeline for article publication

Submit your articles and experience a new surge in publication services
https://www.peertechzpublications.org/submission

Peertechz journals wishes everlasting success in your every endeavours.

Citation: Nalewajski RF (2024) On population-space description of chemical reactivity. Open Journal of Chemistry 10(1): 047-057.
DOI: https://dx.doi.org/10.17352/ojc.000039